



**Estimation of diplodocid length for fragmentary fossils with a 'suspension bridge' (zero-torque) model**

Journal:	<i>Journal of Vertebrate Paleontology</i>
Manuscript ID:	JVP-2009-0013
Manuscript Type:	Article
Date Submitted by the Author:	28-Jan-2009
Complete List of Authors:	Kahn, Philip; UC Berkeley, UC Museum of Paleontology
Key Words:	diplodocidae, biomechanics, mathematical model, torque, least-squares, diplodocus



1  
2  
3 Estimation of diplodocid length for fragmentary fossils with a 'suspension bridge' (zero-torque)  
4  
5 model  
6

7  
8 PHILIP L. KAHN<sup>1</sup>  
9

10  
11  
12 *Note to readers: This is a word document adapted from a LaTeX file. The LaTeX file has the best*  
13 *formatting / readability, but this has been submitted as per requirements for JVP; the TeX file may yet*  
14 *be used for final typesetting.*  
15  
16  
17  
18

19  
20  
21 ABSTRACT – By using simple geometrical arguments, I predict the total length of *Diplodocus*  
22 *carnegii* using a least-squares fit on the cervical series, total dorsal series length, and the height of  
23 the neural spine on vertebra D10. This is done by using a simple, torque-based 'suspension bridge',  
24 or zero-torque, model after using a geometric model to compute neck and tail component masses.  
25 The successful results of this model to *Diplodocus* CM84 and to a recent specimen of *Apatosaurus*  
26 *ajax* suggest that this model is general among diplodocid sauropod dinosaurs. This model therefore  
27 can be used to provide length estimates for fragmentary diplodocid fossils.  
28  
29  
30  
31  
32  
33  
34  
35  
36  
37

38 INTRODUCTION  
39

40 Dinosaur biomechanics can provide insights into the various problems that life encounters  
41 when it reaches massive sizes. Sauropod dinosaurs were the largest known land animals ever to  
42 live, peaking in size around the late Jurassic, and many were built like living 'suspension bridges'  
43 (Alexander 2006). By referring to an animal as a 'suspension bridge', for the purpose of this paper,  
44 I mean a mathematical model that has the primary load-bearing on connective elements  
45 (cables/ligaments) and zero net torque on supporting structures (towers/neural spines). Such  
46 force-balance approaches have been used successfully before (Alexander 1989).  
47  
48  
49  
50  
51  
52  
53  
54  
55

56  
57 <sup>1</sup> University of California Museum of Paleontology, 1101 Valley Life Sciences Building, Berkeley, CA 94720-4780,  
58 pl.kahn@gmail.com  
59  
60

1  
2  
3 In an attempt to model these animals, I examine *Diplodocus carnegii* (Carnegie Museum 84)  
4 and construct a simple mathematical model to predict diplodocid sizes with fragmentary  
5 information. This modeling technique abstracts the form of the dinosaur to simple geometrical  
6 shapes and uses simple physical approximations to predict the length and mass of sauropod necks  
7 and tails that conform to this suspension bridge model, such as diplodocids.  
8  
9

10  
11  
12 To accomplish this, several parameters are needed. The ranges of neck motion have been  
13 modeled for CM 84 by Parrish and Stevens (1999), and those parameters are taken as canonical in  
14 this analysis (Stevens 2002; Stevens and Parrish 2005a). Despite possible problems with the result  
15 as discussed by Upchurch *et al.* (2000), the model constraints provided by the Parrish and Stevens  
16 (1999) analysis are important to this analysis, and the problems are generally limited to those that  
17 should not affect a rigid-body solution. However, the primary reason CM84 was chosen as the test  
18 case is because the animal has comprehensive measurements (Hatcher 1901) for the entire  
19 vertebral series.  
20  
21  
22

23  
24  
25 This approach relies on the value of finding a least-squares linear fit to describe the radius  
26 of cervical vertebrae as a function of distance from the neck. By calculating the mass of bony  
27 elements, the musculature required to move the neck can be calculated, and the mass of the entire  
28 neck follows. The torque that the neck would then apply on dorsal spines can be equated to a  
29 torque that the tail must apply, yielding a quadratic that provides an accompanying tail length.  
30  
31  
32

## 33 34 35 36 37 38 39 40 41 42 43 44 45 METHODS

### 46 47 **Length and Mass Estimates of a *Diplodocus* Neck**

48  
49 By modeling a diplodocid neck as a series of reducing cylinders (of length  $l$  and density  $\rho$ )  
50 and idealizing this to a frustum of a cone, the total mass  $M$  of the neck can be calculated. This model  
51 is shown graphically in Figures 1 and 3. Pneumatic aspects of the skeleton are important to  
52 consider for sauropods, because they are relevant to thermoregulation problems, mass, and oxygen  
53  
54  
55  
56  
57  
58  
59  
60

supply, and are well established in many sauropod lineages (Schwarz and Fritsch 2006; Wedel 2003, 2007). Because the pneumatic features are “virtually identical to those of birds” for all Neosauropoda, pneumaticity is assumed and denoted as  $k_p$  (Wedel 2005). For a description of subscript convention describing body parts, see Figure 1. All variables are used as is standard in physics notation, such as  $m$  for mass,  $\rho$  for volume density,  $r$  for radius,  $l$  for length,  $h$  for height,  $I$  for moment, and  $\tau$  for torque. Capital letters  $M$  and  $L$  are used to represent total mass and length of a part, respectively. Given these assumptions, the total mass of the neck can be described by

$$M = m_t + m_b$$

$$m_b = k_p \int_l^0 \int_0^{r_b} 2\pi\rho_b r(l) dr dl + m_{ns} \quad (1)$$

$$m_{ns} = 2\pi \left( \frac{2}{3} r_b(l) \right)^2 h(l)$$

$$m_t = \int_l^0 \int_{\frac{\pi}{4}}^{\frac{7}{4}\pi} \int_{r_b}^r \rho_t r(l) dr d\theta dl - \int_0^{r_{tr}} 2\pi\rho_{tr} r dr + \int_0^{\frac{\pi}{8} r_t} \int_0^l 2\pi\rho_l r dl dr \quad (2)$$

This construction accounts for the basic morphology of the skeleton, the primary tissue

mass, and an empty column for the trachea. The muscle is treated as leaving a 45° gap at the top of

the cervical vertebrae for ligamentary attachment, which are added separately (Dzemska *et al.* 2007; Organ 2006; Schwarz *et al.* 2007b; Wedel 2002). Based on data from Wedel (2005),  $k_p=0.3$  is taken to be accurate to a first approximation, and assumed to apply to the entire neck. Figure 2 shows that the heights of the neural spines have a very strong linear fit ( $p<10^{-4}$ ) with the distance from the base of the neck, and this least-squares result can be used as the solution to  $h(l)$ . These fits

1  
2  
3 were then taken at the locations of the vertebrae, assumed to have a radius of  $2/3r_b(l)$ , and  
4  
5 computed as a cylinder. This result was then doubled to account for the bifurcated neural spines on  
6  
7 *Diplodocus*.  
8  
9

10 Figure 2 also shows the radius of the cervical vertebrae falls off linearly with length to a  
11 good approximation. Table 1 shows the variation in the linear fitting coefficients for different  
12 selections of vertebrae, for possible representative fragmentary finds. The resulting coefficient  $k_1$   
13 and constant  $k_2$  are for equations of the form  $r(l)=k_1l+k_2$ . The measurements used to calculate these  
14 fits were taken from Hatcher (1901). C1 --- C14 are used for the rest of this analysis due to a high  
15  $|r|$ . The fit using C1, C7 and C15 is left for completeness, but will generally not be practical in the  
16 field, because it would require knowing the distance between the elements before solving.  
17  
18 Nevertheless, the table shows that the fit constant is relatively stable among various choices of  
19 vertebrae, reaching a mean of  $-2.00 \times 10^{-2}$  with a standard deviation of  $\sigma=4.70 \times 10^{-3}$ . Larger fractional  
20 uncertainties occur for fewer vertebrae closer to each other, but the results are nevertheless  
21 consistent among all fit types, with the smallest linear coefficient as 0.93. At four significant figures,  
22 the fit for the first two columns and the fit using C1, C7, and C15 are highly significant ( $p<0.01$ ). The  
23 other two fits fail this test when applied rigorously, with a two-tailed  $p$ -value of 24.5% and 22.9%.  
24  
25 However, this is to be expected with a very small sample size, and the strong other fits suggest that  
26 this degree of correlation should be acceptable in practice. In particular, the fits with a correlation  
27 above 0.95 validate the continuous tapering model as used in Figure 2.  
28  
29  
30  
31  
32  
33  
34  
35  
36  
37  
38  
39  
40  
41  
42  
43  
44  
45  
46  
47

48 There are several possible methods by which the length of the neck can either be  
49 empirically determined or calculated, which is required to calculate the bony core mass and the  
50 moment of inertia. For CM84, the sum of the length of the cervical vertebrae comes to 7.29 m;  
51 however, when the vertebrae are connected and overlap of the centra is taken into account  
52 (neglecting intervertebral discs), a length of 6.7 m is obtained for the cervical series—average for a  
53  
54  
55  
56  
57  
58  
59  
60

1  
2  
3 diplodocid (Hatcher 1901; Stevens and Parrish 2005b; Wedel 2005). With the constants given in  
4  
5 Table 1, it is possible to calculate the length of the neck without actually knowing the entire cervical  
6  
7 series. For example, by choosing a 3 cm final vertebral radius and using the fit from the second  
8  
9 column, the predicted neck length is 7.05 m, which is intermediate between the two methods  
10  
11 detailed above. The choice of a 3 cm minimum radius is based on the radius of the C2 vertebra in  
12  
13 CM84 and an extrapolation from an *Apatosaurus ajax* described by Upchurch *et al.* (2004b). The  
14  
15 worst fit, by using two adjacent vertebrae, under-predicts the neck length by nearly a meter, but  
16  
17 still provides a guideline that is not entirely arbitrary. This method enables only partial cervical  
18  
19 series to be of use in calculating the entire length of the animal, but is not as accurate as direct  
20  
21 measurement from a complete or nearly-complete cervical series. For the purposes of this  
22  
23 treatment, the calculated length  $L=7.05$  m is used.  
24  
25  
26

27 Using a bone density of  $3.16 \text{ g cm}^{-3}$  (treating homogeneous dense bone as  $\text{Ca}(\text{PO}_4)_3\text{OH}$ ), and  
28  
29 a total neural spine mass of  $1.40 \times 10^2 \text{ kg}$ :  
30  
31  
32

$$33 \quad m_b = \rho_b \pi k_b (1.233 \times 10^{-4} l^3 - 1.592 \times 10^{-3} l^2$$

$$34 \quad \quad \quad + 2.742 \times 10^{-2} l) \Big|_{l=7.05} + m_{ns}$$

$$35 \quad \quad \quad \approx 6.09 \times 10^2 \text{ kg}$$

36  
37  
38 If biomechanical limits on neck movement are established, the amount of musculature  
39  
40 required to manipulate the neck on either side can be approximated. The muscle can then be  
41  
42 extended as a column that reduces in radial size as it reaches the cranium.  
43  
44

45 The moment of inertia of the system can be calculated by looking at the torque of the neck  
46  
47 on the lumbar vertebrae. Starting from the definition  $I = \int r^2 dm$ ,  
48  
49  
50  
51  
52  
53  
54  
55  
56  
57  
58  
59  
60

$$\begin{aligned}
 dm &= \pi r(b l)^2 \rho_b dl \\
 &= k_p \rho_b \pi [-0.019l + .166]^2 dl \rightarrow
 \end{aligned}$$

$$I = k_p \rho_b \pi \int_0^l l^2 [-0.019l + 0.166]^2 dl \quad (3)$$

$$\begin{aligned}
 I &= \rho_b \pi k_p (7.40 \times 10^{-5} l^5 \\
 &\quad - 7.96 \times 10^{-4} l^4 + 9.14 \times 10^{-3} l^3) \Big|_{l=7.05} \\
 &\approx 7.52 \times 10^3 \text{ kg}\cdot\text{m}^2 \quad (4)
 \end{aligned}$$

This result is accurate to a first approximation, assuming that each cross-sectional piece is of the same density. Given the assumption that majority of the moment of inertia is supplied by the bone, this approximation is justified because the neck tissues are generally isotropic and homogeneous.

To proceed, the extremes of neck flexion are needed. The movement axis can be rewritten in terms of spherical coordinates, with  $(r, \theta, \phi) = (0, 0, 0)$  at the base of the neck, following mathematical rather than physics conventions (where  $\phi$  is longitudinal). By transforming the Cartesian coordinates of Parrish and Stevens (1999) to spherical coordinates, one obtains a

maximum  $\phi$  range of approximately  $34.9^\circ$  (0.607 rad) and a maximum  $\theta$  of  $43.1^\circ$  (0.752 rad) from

the center, or a total range of  $\Delta\theta \approx 86.17^\circ$  (1.50 rad). This limited vertical range implies the ligament

1  
2  
3 support as modeled in Figure 3 has merit. Using result (4) and the angles through which the neck  
4  
5 moves, the approximate amount of musculature for the neck can be calculated.  
6  
7

8  
9 Here, I take the shoulder girdles to be approximately  $30^\circ$  ( $\pi/6$  rad) off the long axis of the  
10  
11  
12  
13  
14  
15  
16  
17  
18 animal as in Schwarz *et al.* (2007a). The measurement of the coefficient is based on *Diplodocus*  
19  
20 reconstructions but the value of  $r_a$  should not vary much between animals. The muscle attachment  
21  
22 is approximated as occurring over the first meter of the neck, with the posterior end attached at the  
23  
24 scapula and shoulder girdles. The resulting geometry gives a radial distance  $r_a$  from the vertebrae,  
25  
26 which can be used to calculate the torque exerted on the neck by the muscles. Using this value for a  
27  
28 projection reduces the cross product into scalar form.  
29  
30

$$31 \quad r_a \approx 1.240 \cos(\pi/6) + r_b \approx 1.221 \text{ m}$$

32  
33  
34 To complete a calculation of the muscle mass, it is necessary to find the maximum angular  
35  
36 acceleration that the *Diplodocus* head and brain could withstand. If the blood pressure system is  
37  
38 treated as similar to *Giraffa camelopardalis*, it can be feasibly postulated to be capable of handling  
39  
40 up to double standard mammalian blood pressure levels (Hargans *et al.* 1987). Thus a reasonable  
41  
42 solution should be found for a model that treats the maximum acceleration at the head of the  
43  
44 dinosaur to be approximately  $a=3g$  (Seymour and Lillywhite 2000). Using the fact that the torque  
45  
46  $\tau=a|I|$ ,  
47  
48  
49  
50  
51  
52  
53  
54  
55  
56  
57  
58  
59  
60



$$\begin{aligned}
 \tau &= 3g|I| \\
 &= F \int_0^1 r \sin \left( \arctan \left( \frac{r_a}{r} \right) \right) dr \\
 &= Fr_a r \sqrt{\frac{r_a^2}{r^2} + 1} \Big|_{r=1} \rightarrow \quad (5)
 \end{aligned}$$

$$\begin{aligned}
 F &= \frac{3g|I|}{r_a \sqrt{r_a^2 + 1}} \quad (6) \\
 &\approx 1.06 \times 10^5 \text{ N}
 \end{aligned}$$

Taking this as the maximum force required to swing the base of the neck, the resulting arc

can be extended over a 43.1° lateral rotation as by Parrish and Stevens (1999) resulting in a work

output of:

$$(1.06 \times 10^5 \text{ N})(1 \text{ m})(0.752 \text{ rad}) = 7.97 \times 10^4 \text{ J}$$

Given that the mean power output of muscle is approximately 1 kW·kg<sup>-1</sup>, this then yields

67.9 kg·s<sup>-1</sup> of muscle required to accelerate the neck for any length of time  $t$  (Alexander 2002). It is

1  
2  
3 simple to show the maximal rotational velocity occurs in  $t=\sqrt{(2L\theta/a)}\approx 0.607$  seconds, resulting in  
4  
5 approximately 49.9 kg of muscle required to swing the neck in a given direction.  
6

7 To complete the analysis, this base muscle-mass result must be multiplied by two to  
8  
9 account for both sides of the neck. This calculation can be repeated for the top and bottom of the  
10  
11  
12  
13  
14 neck, substituting the appropriate angle terms. Substituting in a density of  $\rho_m\approx 1050$  kg·m<sup>-3</sup>, this  
15  
16  
17  
18  
19  
20  
21  
22 yields  $m_m\approx 1.47\times 10^2$  kg (Alexander 2002).  
23  
24  
25  
26

27 Using a mean ligament density of  $\langle\rho_l\rangle\approx 1$  g·cm<sup>-3</sup>=1000 kg·m<sup>-3</sup>, and tracheal radius  $r_{tr}$ , the total  
28  
29  
30  
31  
32  
33  
34

35 neck tissue mass can be represented by  
36  
37

$$m_t \approx m_m - \pi r_{tr}^2 l + \int_0^l \frac{\pi^2}{8} r_t l \rho_l dl \quad (7)$$

38  
39  
40  
41  
42 Stretching the tissue across the neck in a partial cylindrical shell (as Figure 1),  
43  
44

$$m_m = \rho_t l \frac{7}{8} \pi (r_t(l) - r_b(l))^2 \rightarrow$$

$$r_t(l) = \sqrt{\frac{8m_m}{7\pi}} + r_b(l) \quad (8)$$

45  
46  
47  
48  
49  
50  
51  
52 Which can be substituted into the final integral term in Equation 7 to calculate the  
53  
54  
55 ligamentary mass:  
56  
57  
58  
59  
60

$$m_l = \frac{\pi^2 \rho l}{8} \int_0^l l \sqrt{\frac{8m_m}{7\pi}} - lr_b(l) dl \quad (9)$$

$$\approx 2.22 \times 10^2 \text{ kg} \quad (10)$$

Finally, it is assumed that the trachea has a radius about equal to that of the C2 vertebra, or .027 m (Hatcher 1901), giving:

$$\begin{aligned} m_t &\approx m_m - \pi r_{tr}^2 l + m_l \\ &\approx 3.33 \times 10^2 \text{ kg} \end{aligned}$$

For a total neck mass of  $M=5.85 \times 10^2 + 3.04 \times 10^2 = 9.77 \times 10^2$  kg for a *Diplodocus* neck --- an upper bound of 8.1% of its total mass (Henderson 2003). This result neglects the mass of the head, which would have to weigh over 40 kg to result in a 5% correction.

### Estimating Sauropod Tail Length

Estimation of *Diplodocus*' tail length can be accomplished by using a "suspension bridge" design to the lumbar neural spines and by applying a similar mass analysis to the one just performed on the neck. Solving for a net zero torque on thoracic and lumbar neural spines can then yield a predicted tail length. This is an oversimplification of ligamentary attachment along the vertebrae, but accurate to a first approximation, and such a force-balance approach has precedent, and prior work has shown elastic ligaments would be strong enough to support the neck (Alexander 1989, 2006; Schwarz *et al.* 2007b).

For the sake of simplicity, it is assumed that a single ligament connects the highest neural spine over the acetabulum to the middle of its neck, with that neural spine supporting the entire torque of the neck. The neck and tail is supported at its center of mass,  $L/4$ . This is then equated to the torque placed on the same neural spine by the tail; that is,  $\tau_{neck} - \tau_{tail} = 0$ . It is this equality that prompted the mass of the neck to be calculated previously.

The tail radius as a function of length is

$$r_T(l) = \frac{R_f - R_i}{L_T} l + R_i$$

Where  $R_i$  is the initial radius at the base of the tail,  $R_f$  the final radius at its extremum,  $L$  its total length, and  $l$  the position of an element along its length. For convenience,  $\eta \equiv R_f - R_i$ . In these calculations, the values are known from Hatcher (1901); however, even for incomplete specimens these values should not be difficult to extrapolate.

Rewriting Equations 1 and 3,

$$m_{bT} = \rho_b k_{pt} \pi \int_0^L r_T(l)^2 dl$$

$$I_T = \rho_b k_{pt} \pi \int_0^L r_T(l)^4 dl$$

Leading to

$$m_{bT} = \rho_b k_{pt} \pi \left( \frac{1}{2} \eta^2 + \eta R_i + R_i^2 \right) \quad (11)$$

$$I_T = \rho_b k_{pt} \pi \left( \frac{1}{4} \eta^4 + \eta^3 R_i + 2\eta^2 R_i^2 + 2\eta R_i^3 + R_i^4 \right) \quad (12)$$

Since current tail reconstructions suggest an only partially pneumatic tail (such as Wedel (2005)), here I assume that approximately 75% of the tail is fully pneumatic, and the rest of the tail is apneumatic, instead of the reducing pneumaticity toward the posterior end of the tail. This results in a mean pneumaticity of  $k_{pt} \approx 0.53$ . This results in a tail bone mass of  $m_b \approx 2.97 \times 10^2$  kg and a moment of inertia of  $2.87 \times 10^2$  N·m.

1  
2  
3 To proceed, the assumption is made that the extremum of the tail can break the speed of  
4  
5  
6  
7  
8 sound ( $c_s=343 \text{ m}\cdot\text{s}^{-1}$  at 293 K) as suggested by Mhyrvold and Currie (1997). Assuming the tail  
9  
10  
11  
12  
13  
14  
15  
16  
17  
18 reaches 110%  $c_s$  ( $v_{ss}=377.3 \text{ m}\cdot\text{s}^{-1}$ ) over a quarter rotation of the available range,  
19  
20  
21  
22  
23  
24  
25  
26

$$\begin{aligned}
 \tau_w &= I\alpha \\
 &= 2I_T vt^{-1} \\
 &= \frac{2I_T v^2}{L_T \sin \pi/8}
 \end{aligned}$$

27  
28  
29  
30  
31  
32  
33  
34 This can then be substituted into a force-torque equation, as in Equation 5. The joule-  
35  
36 kilograms expended is  $F\theta_{ss}$ , where  $\theta_{ss}$  is the angle through which the tail rotates in this time frame  
37  
38  
39  
40  
41 ( $\pi/8$  rad, or  $27.5^\circ$ ).  
42  
43  
44  
45  
46  
47  
48  
49  
50  
51  
52  
53  
54  
55  
56  
57  
58  
59  
60

The product of the energy, elapsed time, and the mean power output of muscle  $4Et\langle P_m \rangle$

results in

$$\begin{aligned}
 m_{mT} &= \left( \frac{4L \sin(\pi/8)}{10^3 v_{ss}} \right) \left( \frac{2|I_T| v_{ss}^2}{L_T \sin(\pi/8)} \right) \phi_{ss} \\
 &\quad \left( R_i \sqrt{R_i^2 + 1} \right)^{-1} \\
 &= \frac{|I_T| |v_{ss}|}{125 R_i \sqrt{R_i^2 + 1}} \phi_{ss} \quad (13) \\
 &\approx 9.03 \times 10^2 \text{ kg} \\
 M_T &= m_{bT} + m_{mT} + m_l \frac{m_{bT} + m_{mT}}{M}
 \end{aligned}$$

The final term in the total mass is a correction for the ligaments holding the tail, where they are assumed to be scaled linearly with the mass ratio of the rest of the tail components to the neck. The forces and torques can be set up as illustrated in Figure 4. With the ligament modeled to be connected to the middle of the tail, the model results in  $\tan \theta = 4h/L_p$ , and  $F_y = mg \sin \theta$ . The hypotenuse and overall force are

$$\begin{aligned}
 r &= \sqrt{(L_d + L_p/4)^2 + h^2} \\
 F_y &= Mg \sin \left( \arctan \left( \frac{4h}{L_p} \right) \right)
 \end{aligned}$$

Where  $L_d$  is the dorsal vertebra distance to the acetabulum,  $h = \Delta h + h_{ns}$  the vertical offset to the neutral position as shown in Figure 4.  $L_p$  is used to show that this can be used for either the neck or the tail, and the correct value can be input / calculated for as required by context.  $D_n$  as a variable will also represent the length of the  $n$ th dorsal vertebra. In context,  $L_d = D_{11}$  for the tail, and the sum of dorsals 1-9 for the neck.

The torque of the neck can be explicitly solved with its calculated values of  $M$  and  $L$ , model value  $\Delta h=0$ , the estimated or known height of the tallest neural spine  $h_{ns^*}$ , and  $L_d=\sum_{n=1}^9 D_n$ . The resulting  $\tau_n$  can then be equated with the same equation from the tail:

$$\begin{aligned}\tau_n &= 2.22 \times 10^4 \text{ N} \cdot \text{m} \\ &= M_T g \left( (L_d + L_T/4)^2 + h_T^2 \right)^{1/2} \sin \left( \arctan \left( \frac{4h_T}{L_T} \right) \right)\end{aligned}$$

Squaring, taking a small angle approximation, and expanding,

$$(L_d^2 + L_T L_d + h_T^2) \left( \frac{4h_T}{L_T} \right)^2 + h_T^2 \approx \left( \frac{\tau_n}{M_T g} \right)^2$$

Reducing to the quadratic in  $L$ :

$$\left( h_T^2 - \left( \frac{\tau_n}{M_T g} \right)^2 \right) L_T^2 + 8h_T^2 L_d L_T + 16 (L_d^2 h_T^2 + h_T^4) = 0 \quad (14)$$

Applying the quadratic formula, and using  $L_d=D_{11}=0.270$  m and approximating  $\Delta h_T=1.25$  m (Hatcher 1901), the physical solution to the equation is then a tail length of 16.7 m and mass of  $1.47 \times 10^3$  kg. Summing this up with the other known lengths of the body parts, the model obtains a total animal length of 28.6 m, or within about 4.3% removed from the length of the current restoration at 27.4 m.

## Summary

By finding a least-squares linear fit for the neck ( $r(l)$ ), extrapolating to a minimum radius, the following combined equations from the Methods section can be solved in order to calculate the length and the masses of both the neck and tail of a diplodocid.

$$I = k_p \rho_b \pi \int_0^l l^2 r_b(l)^2 dl \quad (15)$$

$$m_m = \frac{|I|}{r_a} \sqrt{\frac{6gL}{r_a^2 + 1}} \left( \theta_{horiz}^{3/2} + \theta_{vert}^{3/2} \right) \quad (16)$$

$$M = m_m - \pi r_{tr}^2 l + \frac{\pi^2 \rho_l}{8} \int_0^l l \sqrt{\frac{8m_m}{7\pi}} - l r_b(l) dl \quad (17)$$

$$\tau_n = Mg \sin \left( \arctan \left( \frac{4h_{ns*}}{L} \right) \right) \left( \sqrt{(L_d + L/4)^2 + h_{ns*}^2} \right) \quad (18)$$

$$m_{bT} = \rho_b k_{p_i} \pi \left( \frac{1}{2} \eta^2 + \eta R_i + R_i^2 \right) \quad (19)$$

$$I_T = \rho_b k_{p_i} \pi \left( \frac{1}{4} \eta^4 + \eta^3 R_i + 2\eta^2 R_i^2 + 2\eta R_i^3 + R_i^4 \right) \quad (20)$$

$$M_T = \frac{\pi |I_T| |v_{ss}|}{10^3 R_i \sqrt{R_i^2 + 1}} + m_l \frac{m_{bT} + m_{mT}}{M} + m_{bT} \quad (21)$$

$$0 = \left( h_T^2 - \left( \frac{\tau_n}{M_T g} \right)^2 \right) L_T^2 - 8h^2 L_d L_T - 16 (L_d^2 h_T^2 + h_T^4) \quad (22)$$

This model then requires in addition only the length of the dorsal series, scapular girdle, initial tail radius, and vertical tail offset.

## DISCUSSION

Based on the results generated by the physical model, his method of modeling length can be generalized to various sauropods. The accuracy of the results can always be increased; for the mass of the skeleton, the neck can be better modeled by using a function that would give a better approximation to the shape of the cervical vertebrae, and the tapering of the neck can always be better approximated by a nonlinear expression. The tissue mass can be better approximated by



1  
2  
3 breaking it into the sums of integrals over particular muscle groups (instead of a single group over  
4 the first meter), and the ligaments can be better treated by having a separate set of expressions for  
5 them, and modeling where and how the ligaments connect in a more rigorous fashion. Practically,  
6 however, the results given are more than sufficient in accuracy. The most influential factors in the  
7 result are the pneumaticity factors and the precise fit used. Whereas any cervical vertebra series  
8 may be used here, the longest continuous series starting close to the base of the neck will generally  
9 return the best fits.

10  
11 The tendency of this solution is to over-estimate the mass; insufficient modeling of the  
12 vertebrae gives them more volume than they actually had. This over-estimation of mass will tend  
13 to decrease animal size if biased toward the head, and increase animal size if biased toward the tail.  
14 Finally, calculating musculature based on a maximum head and tail velocity might be problematic,  
15 but was the most limiting case available.

16  
17 Both the neck and the tail are taken to be  $\theta$  independent, and the calculations only have  
18 neural spine data added at the end, which are treated separately. The bifurcated cervical spines are  
19 treated as a single element for simplicity. The  $k_p$  factor that appears is 1-ASP or a variation on the  
20 “Airspace Proportion” proposed by Wedel (2005). This treatment also assumes that the density of  
21 the tracheal space is negligible; that is,  $\rho_{air} \approx 1.3 \text{ mg/cc} \rightarrow 0$ .

22  
23 The modeling of the tail could be improved by using more than an “average” ligamentary  
24 connection, and providing proper connective chains of the ligaments rather than a rigid-model  
25 approximation. Additionally, the ligaments could be separately accounted for. However, this runs  
26 contrary to the goal of this paper in constructing a low-order polynomial solution that can be  
27 quickly done on a calculator. The  $k_p$  for the tail used is in line with approximate values that can be  
28 obtained from the Wedel's (2005) analysis. There, Wedel calculates an approximate mass savings  
29 of 300 kg for the caudal series, which, for a 600 kg apneumatic tail, represents a tail  $k_{pT} \approx 0.5$ , in line  
30 with the “75%” estimate used here.

1  
2  
3 The pneumaticity of the axial skeleton is interesting to note here. The combined mass of the  
4 tail and the neck --- which comprises the majority of the length of the animal --- comprises at most  
5 22% the mass of the total body as calculated by Henderson (2003). Additionally, the fact that these  
6 measurements of pneumaticity are required to predict sizes of the animal provides an additional  
7 method by which one can obtain pneumaticity estimates. "Bogus" estimates of pneumaticity result  
8 only in nonphysical solutions to the quadratic.  
9  
10  
11  
12  
13  
14  
15

16 To ensure the result was not a coincidence, the analysis was performed on the incomplete  
17 neck of a "medium-sized" *Apatosaurus ajax* (NSMT-PV 20375) described by Upchurch *et al.*  
18 (2004b).  $\Delta h_T$  was obtained by adding the last dorsal and sacral vertebra's radii, CM84's neural  
19 spine mass was used, the tail and the fit obtained with C3---C9.  $k_p$  was based on cervical  
20 midcentrum measurements and  $k_{pt}$  used the "75%" estimate with respect to the cervical condyle  
21 (Wedel 2005). This resulted in a very typical total length of 22.0 m, suggesting that the applicability  
22 to *Diplodocus* is unlikely to be a chance artifact.  
23  
24  
25  
26  
27  
28  
29  
30  
31  
32  
33

### 34 CONCLUSION

35  
36 The approximations and type of solutions done in this paper only apply to sauropods whose  
37 biomechanics can be described as similar to a suspension bridge, such as diplodocids. Currently, I  
38 propose no method by which the length of the dorsal series can be estimated with only fragmentary  
39 finds, and the requirement of this as the variable  $L_d$  makes this the most strongest requirement of  
40 specimen completeness. In a broader context, the results of this study would suggest that because a  
41 zero-torque model predicts diplodocid length with high-precision, it is likely this model which was  
42 the primary enabling feature that allowed sauropods to reach their massive sizes.  
43  
44  
45  
46  
47  
48  
49  
50

51 Future work would include brachiosaurids, juvenile diplodocids, titanosaurids, and oddly  
52 proportioned members of Sauropoda that should otherwise conform to this model. Many of these  
53 would require fairly significant changes to the model, and sauropods that are not based on a zero-  
54  
55  
56  
57  
58  
59  
60

1  
2  
3 torque model, such as *Brachiosaurus*, will fail to have reasonable predictions. Smaller animals such  
4  
5 as juveniles would not obey the assumptions made about speed of the tail and neck. There are  
6  
7 interesting candidates that would test the assertion made here that the massive head should not be  
8  
9 significant (such as *Dicraeosaurus*) and the predictive abilities of this method on oddly-  
10  
11 proportioned individuals such as *Mamenchisaurus*. Finally, titanosaurids are more roust and not  
12  
13 traditionally thought of as “living suspension bridges”. However, these are diverse enough in  
14  
15 methods and significant enough changes to warrant a separate treatment. The changes required  
16  
17 are validated by a direct application of this theory to a juvenile diplodocid (SMA 0009) described in  
18  
19 Schwarz *et al.* (2007c), in which constants assumed for adult animals yield nonphysical ligamentary  
20  
21 masses.  
22  
23  
24  
25  
26

#### 27 ACKNOWLEDGMENTS

28  
29 I thank K. Padian, M. Wedel, and S. Werning for their assistance in writing and correcting  
30  
31 this paper, and for ensuring that I did not leave important biology unaccounted for. I also thank K.  
32  
33 Honjo and S. Kaufman for their assistance in proofreading and encouragement. (Editors and  
34  
35 reviewers, by name). Finally, I thank K. Colwell who spent many hours with me making sure my  
36  
37 math and modeling parameters were correct, and S. Weinstein, who probably proof-read this paper  
38  
39 more than everyone else put together.  
40  
41  
42  
43  
44

#### 45 REFERENCES

- 46  
47 Alexander, R. M. 1989. Mechanics of fossil vertebrates: William Smith lecture. Journal of the  
48  
49 Geological Society, London 146:1--52. doi: 10.1144/gsjgs.146.1.0041.  
50  
51 Alexander, R. M. 2002. Tendon elasticity and muscle function. Comparative Biochemical Physiology,  
52  
53 A 133:1001--1011. doi: 10.1016/S1095-6433(02)00143-5.  
54  
55  
56  
57  
58  
59  
60

- 1  
2  
3 Alexander, R. M. 2006. Dinosaur Biomechanics. *Proceedings of the Royal Society B* 273:1849--  
4  
5 1855. doi: 10.1098/rspb.2006.3532.  
6  
7  
8 Dzemski, G., and A. Christian. 2007. Flexibility along the neck of the ostrich (*Struthio camelus*) and  
9  
10 consequences for the reconstruction of dinosaurs with extreme neck length. *Journal of*  
11  
12 *Morphology* 268:701--714. doi: 10.1002/jmor.10542.  
13  
14 Hargans, A. R., R. W. Millard, K. Pettersson, and K. Johansen. 1987. Gravitational haemodynamics  
15  
16 and oedema prevention in the giraffe. *Nature* 329:59--60. doi: 10.1038/329059a0.  
17  
18  
19 Hatcher, J. B. 1901. *Diplodocus: Its osteology, taxonomy, and probable habits, with restoration of*  
20  
21 *its skeleton*. The Carnegie Institute, Washington, DC.  
22  
23  
24 Henderson, D. M. 2003. Topsy punters: Sauropod dinosaur pneumaticity, buoyancy, and aquatic  
25  
26 habits. *Proceedings of the Royal Society B* 271:180--183. doi: 10.1098/rsbl.2003.0136.  
27  
28  
29 Mhyrvold, N., and P. Currie. 1997. Supersonic sauropods? Tail dynamics in the diplodocids.  
30  
31 *Paleobiology* 23:393-409.  
32  
33  
34 Organ, C. L. 2006. Thoracic epaxial muscles in living archosaurs and ornithopod dinosaurs. *The*  
35  
36 *Anatomical Record Part A: Discoveries in Molecular, Cellular, and Evolutionary Biology*  
37  
38 288:782--793. doi: 10.1002/ar.a.20341.  
39  
40  
41 Parrish, J. M., and K. A. Stevens. 1999. Neck posture and feeding habits of two Jurassic sauropod  
42  
43 dinosaurs. *Science* 284:98—800. doi: 10.1126/science.284.5415.798.  
44  
45  
46 Schwarz, D., E. D. Frey, and C. A. Meyer. 2007a. Novel reconstruction of the orientation of the  
47  
48 pectoral girdle in sauropods. *Anatomical Record B* 290:32--47. doi: 10.1002/ar.20405.  
49  
50  
51 Schwarz, D., E. D. Frey, and C. A. Meyer. 2007b. Pneumaticity and soft-tissue reconstructions in the  
52  
53 neck of diplodocid and dicraeosaurid sauropods. *Acta Palaeontologia Polonica* 52:167--  
54  
55 188.  
56  
57  
58  
59  
60

- 1  
2  
3 Schwarz, D. , and G. Fritsch. 2006. Pneumatic structures in the cervical vertebrae of the late Jurassic  
4  
5 Tendaguru sauropods *Brachiosaurus branchai* and *Dicraeosaurus*. *Ecologiae Geologicae*  
6  
7 *Helvetica* 99:65--78. doi: 10.1007/s00015-006-1177-x.  
8  
9
- 10 Schwarz, D., T. Ikejiri, B. H. Breithaupt, and P. M. Sander. 2007c. A nearly complete skeleton of an  
11  
12 early juvenile diplodocid (Dinosauria: Sauropoda) from the Lower Morrison Formation  
13  
14 (Late Jurassic) of north central Wyoming and its implications for early ontogeny and  
15  
16 pneumaticity in sauropods. *Historical Biology* 19:225--253.  
17  
18 doi:10.1080/08912960601118651.  
19
- 20  
21 Seymour, R. S., and H. B. Lillywhite. 2000. Hearts, neck posture, and metabolic intensity of sauropod  
22  
23 dinosaurs. *Proceedings of the Royal Society B* 267:1883--1887.  
24  
25 doi:10.1098/rspb.2000.1225.  
26
- 27  
28 Stevens, K. A. 2002. Dinomorph: Parametric modeling of skeletal structures. *Senckenbergiana*  
29  
30 *Lethaea* 82:23--34.  
31
- 32  
33 Stevens, K. A., and J. M. Parrish. 2005a. Digital Reconstructions of Sauropod Dinosaurs and  
34  
35 Implications for Feeding; pp178--200 in K. C. Rogers (ed.) and J. Wilson (ed.), *The*  
36  
37 *Sauropods: Evolution and Paleobiology*. University of California Press, Berkeley and Los  
38  
39 Angeles.  
40
- 41  
42 Stevens, K. A., and J. M. Parrish. 2005b. Neck posture, dentition, and feeding strategies in Jurassic  
43  
44 sauropod dinosaurs; pp212--232 in V. Tidwell (ed.) and K. Carpenter (ed.), *Thunder-*  
45  
46 *lizards: The Sauropodomorph Dinosaurs*. Indiana University Press, Bloomington.  
47
- 48  
49 Upchurch, P., K. A. Stevens, and J. M. Parrish. 2000. Technical comment: Neck posture of sauropod  
50  
51 dinosaurs. *Science* 287:547. doi: 10.1126/science.287.5453.547b.  
52
- 53  
54 Upchurch, P., P. M. Barrett, and P. Dodson. 2004. Sauropoda; pp316--318 in D. B. Weishampel (ed.),  
55  
56 P. Dodson (ed.), and H. Osmólska (ed.), *The Dinosauria*, 2nd edn. University of California  
57  
58 Press, Berkeley and Los Angeles.  
59  
60

1  
2  
3 Upchurch, P., Y. Tomida, and P. M. Barrett. 2004. A new specimen of *Apatosaurus ajax* from the  
4 Morrison formation (Upper Jurassic) of Wyoming, USA. National Science Museum  
5 monographs 26:pp. i--118.  
6  
7

8  
9  
10 Wedel, M. J. 2003. Vertebral pneumaticity, air sacs, and the physiology of sauropod dinosaurs.  
11  
12 Paleobiology 29:243--255.  
13  
14 doi: 10.1666/0094-8373(2003)029\$<\$0243:VPASAT\$>\$2.0.CO;2.  
15

16  
17 Wedel, M. J. 2005. Postcranial skeletal pneumaticity in sauropods and its implications for mass  
18 estimates. pp201--228 in K. C. Rogers (ed.) and J. Wilson (ed.), *The Sauropods: Evolution*  
19 *and Paleobiology*. University of California Press, Berkeley and Los Angeles.  
20  
21

22  
23 Wedel, M. J. 2007. Postcranial pneumaticity in dinosaurs and the origin of the avian lung. Ph.D.  
24  
25 dissertation, University of California, Berkeley, California, 304pp.  
26

27  
28 Wedel, M. J., and R. K. Sanders. 2002. Osteological correlates of cervical musculature in aves and  
29  
30 sauropoda (dinosauria: saurischia), with comments on the cervical ribs of *Apatosaurus*.  
31  
32 Paleobios 22:1-6.  
33

34 Submitted January 28, 2009; accepted Month, DD, YYYY.  
35  
36  
37  
38  
39  
40  
41  
42  
43  
44  
45  
46  
47  
48  
49  
50  
51  
52  
53  
54  
55  
56  
57  
58  
59  
60

1  
2  
3  
4  
5  
6  
7  
8  
9  
10  
11  
12  
13  
14  
15  
16  
17  
18  
19  
20  
21  
22  
23  
24  
25  
26  
27  
28  
29  
30  
31  
32  
33  
34  
35  
36  
37  
38  
39  
40  
41  
42  
43  
44  
45  
46  
47  
48  
49  
50  
51  
52  
53  
54  
55  
56  
57  
58  
59  
60

FIGURE 1. A cross-sectional schematic of the model neck construction. The elements identified here are subscripted in equations by  $b$  for the bone,  $l$  for the ligaments,  $m$  for muscle mass,  $ns$  for the neural spines,  $t$  for tissue mass, and  $tr$  for the trachea. The capital subscript  $T$  is added when these variables refer to the tail. For a side-schematic view, see Figure 3. Vertebrae taken from Hatcher (1901), plate VI.

FIGURE 2. Plots of  $O(4)$  and linear fits for the cervical series, and a linear fit for the neural spine heights. The dotted line is the complete least squares fit, the solid line the one neglecting the base cervical. It is this fit that is used in the text. The neural spine fit has  $h(l)=-5.82\times 10^{-2}l+0.61$ , a maximum fractional uncertainty of 4.21%, and  $r=0.99$ .

FIGURE 3. Side schematic view of model, reflecting neck tapering in model. The top image is a silhouette CM84, and the bottom image the proposed model.

FIGURE 4. Schematic of force setup on the tail as used to begin the torque-balance equations. The setup is analogous for the neck, with the neutral point of torque chosen to be large neural spines above the acetabulum.

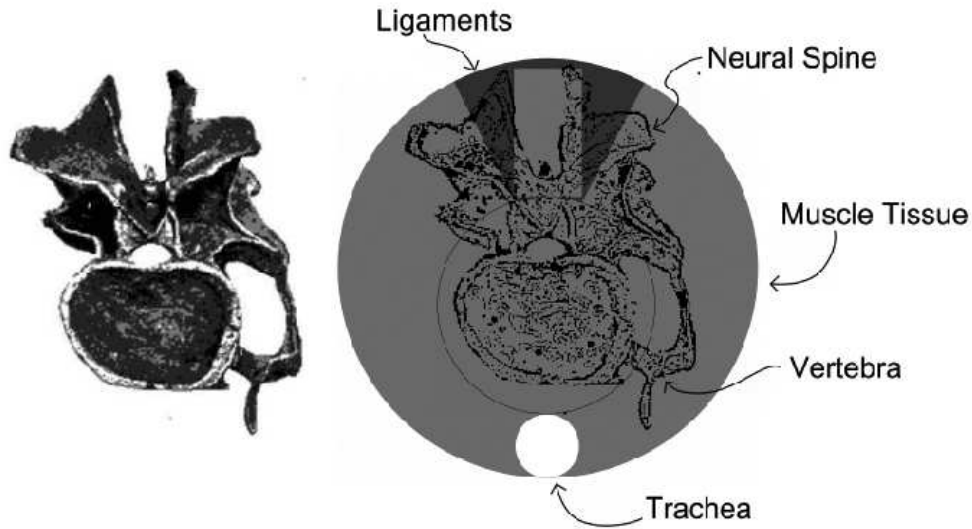
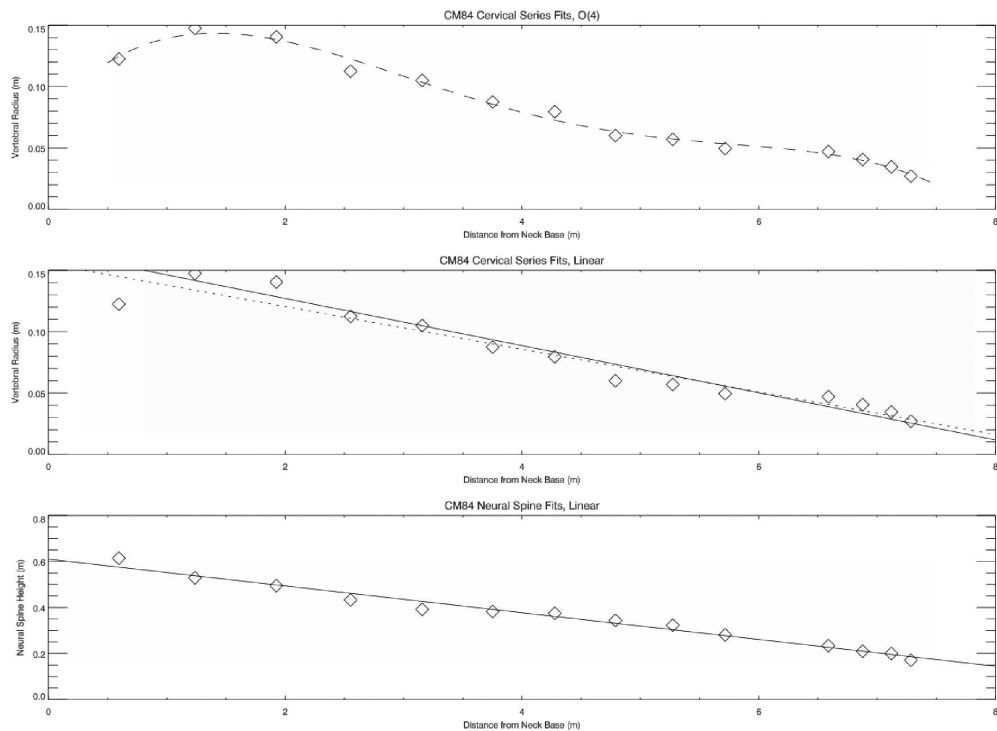


Figure 1. A cross-sectional schematic of the model neck construction. The elements identified here are subscripted in equations by  $b$  for the bone,  $l$  for the ligaments,  $m$  for muscle mass,  $ns$  for the neural spines,  $t$  for tissue mass, and  $tr$  for the trachea. The capital subscript  $T$  is added when these variables refer to the tail. For a side-schematic view, see Figure 3. Vertebrae taken from Hatcher (1901), plate VI.

58x39mm (300 x 300 DPI)





Plots of  $O(4)$  and linear fits for the cervical series, and a linear fit for the neural spine heights. The dotted line is the complete least squares fit, the solid line the one neglecting the base cervical. It is this fit that is used in the text. The neural spine fit has  $h(l) = -5.82 \times 10^{-2}l + 0.61$ , a maximum fractional uncertainty of 4.21%, and  $r = 0.99$ .

182x132mm (300 x 300 DPI)

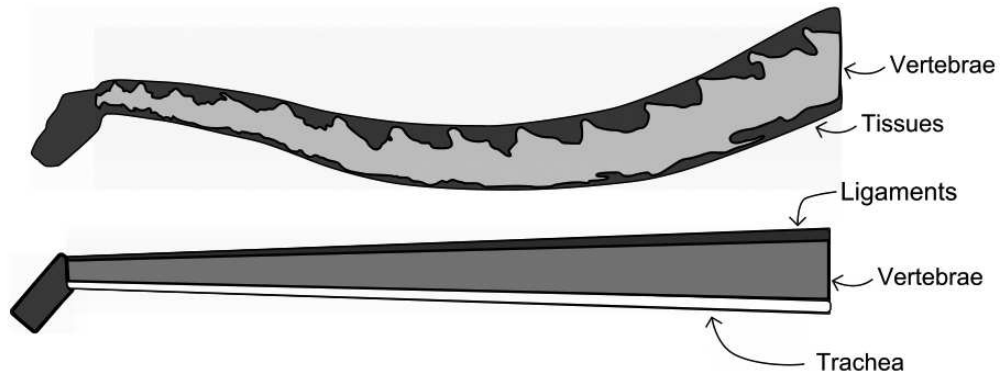


Figure 3. Side schematic view of model, reflecting neck tapering in model. The top image is a silhouette CM84, and the bottom image the proposed model.  
77x29mm (300 x 300 DPI)

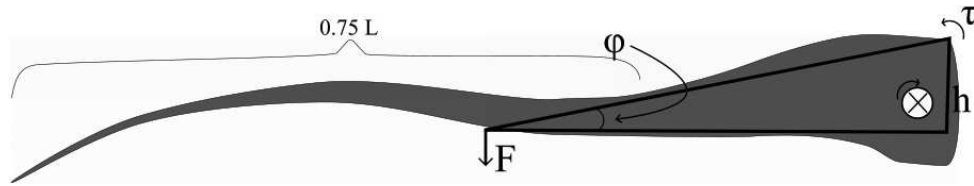


Figure 4. Schematic of force setup on the tail as used to begin the torque-balance equations. The setup is analogous for the neck, with the neutral point of torque chosen to be large neural spines above the acetabulum.  
79x17mm (300 x 300 DPI)

Table 1. Taper coefficients and constant offset for various methods of measurement. Uncertainty is the maximum fractional uncertainty,  $|r|$  is the correlation coefficient.

	C1 – C15	C1 – C14	C6 – C8	C1, C7 and C15	C2 – C4
Constant $k_1$	$-1.74 \times 10^{-2}$	$-1.92 \times 10^{-2}$	$-2.27 \times 10^{-2}$	$-1.42 \times 10^{-2}$	$-2.64 \times 10^{-2}$
Offset $k_2$	$1.55 \times 10^{-1}$	$1.66 \times 10^{-1}$	$1.74 \times 10^{-1}$	$1.31 \times 10^{-1}$	$1.84 \times 10^{-1}$
Uncertainty	7.62%	5.72%	40.51%	1.49%	37.67%
$ r $	0.97	0.98	0.93	1.00	0.94